

# A Comparison of Finite vs. Infinite Plane Models of Reference Conductors in Electronic Packages

Yi-Ru Jeong and Ali E. Yilmaz

Department of Electrical and Computer Engineering, The University of Texas at Austin, Austin, Texas, USA  
yiruta@utexas.edu, ayilmaz@mail.utexas.edu

**Abstract**—The accuracy of two layered-medium integral-equation approaches are evaluated using a benchmark package-scale microstrip line: (i) In the typical approach, where dielectric layers are extended to infinity using Green’s functions, the currents in/on all conductors (here, a signal line and ground plane) are discretized. (ii) In the reduced-domain approach, where large reference conductors are also extended to infinity using Green’s functions, the currents in/on a reduced set of conductors (here, only the signal line) are discretized. The approaches are contrasted by computing network parameters of the microstrip line using lumped-port models and diminishing port-truncation effects using a de-embedding technique. It is shown that the S11 parameter found by the typical approach is highly sensitive to the ground-plane mesh density under the signal line and requires finer meshes to reach to the accuracy of the reduced-domain approach.

**Keywords**—Integral-equation methods; layered media.

## I. INTRODUCTION

Reduced-domain layered-medium integral equation (LMIE) approaches can enable accurate, rapid, and scalable electromagnetic simulations of modern electronic packages [1]. In these approaches, the number of unknowns is reduced beyond that of the typical LMIE methods by extending large reference conductors (e.g., ground/power planes) to infinity and incorporating them into the Green’s functions. While zero-thickness perfectly-conducting layers are commonly used in reduced-domain LMIE methods [2],[3], finite-thickness highly-conducting layers can also be used to more accurately model finite-thickness, finite-conductivity, and surface-roughness effects on reference conductors [1]. Because they discretize the current in/on a reduced set of conductors, such LMIE methods can result in smaller and better-conditioned [1] systems of equations.

In this article, a reduced-domain LMIE method is contrasted to a typical LMIE method by using them to compute the network parameters of a package-scale benchmark microstrip line. Significant differences are observed when the S11 parameters found by the two are compared, even after a de-embedding technique is used to reduce the port discontinuity effects. To investigate the origin of the differences, the results are compared as increasingly finer meshes are used. It is observed that as the mesh density increases, the difference between the de-embedded results decreases and that the reduced-domain LMIE shows more accurate results than the typical LMIE for the same mesh density on the signal line. The differences and the less accurate parameters found by the typical LMIE approach are attributed to the numerical solution rather than analytical modeling via the Green’s functions of the currents on the ground plane.

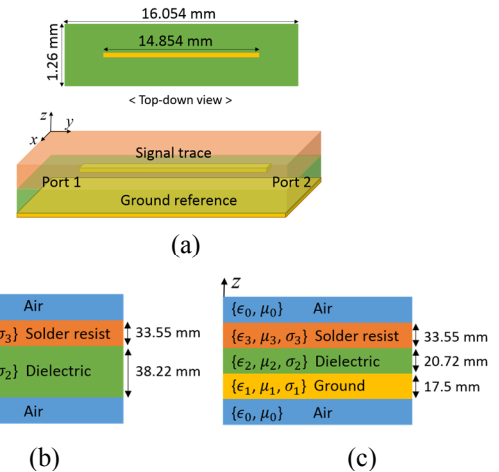


Fig. 1. (a) Top-down and 3-D view of the microstrip line structure. (b) A 4-layer background model for the typical LMIE method [4]. (c) A 5-layer background model for the reduced-domain LMIE method [1].

## II. NUMERICAL METHOD

Consider the two different background models of the benchmark microstrip line from [1],[4] shown in Fig. 1. In the typical LMIE approach, the signal line and ground conductors are modeled as residing in a 4-layer planar stratified medium (Fig. 1(b)). In the reduced-domain LMIE approach, only the signal line is modeled as residing in a 5-layer planar stratified medium (Fig. 1(c)) and the reference conductor is modeled as an infinite layer of finite thickness and conductivity. The material parameters of the different layers can be found in [1]. In both LMIE approaches, the surfaces of the conductors that are not modeled as part of the background medium are meshed using triangles (Fig. 2); the surface current density on these conductors is approximated using RWG functions [5]; and impedance-boundary conditions are enforced on these surfaces. Non-radiating lumped-port models are used to extract the network parameters as detailed in [1],[4],[8].

### A. Typical LMIE Approach

Layered-medium Green’s functions are computed numerically from Sommerfeld integrals with asymptotic-term subtraction scheme and interpolation from sampled results [4],[6],[7]. While dielectric layers are included in the Green’s function computation, conductors for the signal traces and the ground reference are meshed as both are modeled as finite-thickness finite-sized conductors. Generally, the unknowns on the reference conductor constitute a significant portion of the total number of unknowns (Fig. 2).

### III. INFINITE VS. FINITE GROUND MODEL

The microstrip line is analyzed using the typical and reduced-domain LMIE methods to evaluate the differences between finite and infinite ground models. To investigate the accuracy and convergence of the methods, the three kinds of meshes shown in Figs. 2 (a)-(c) are used: (i) In the normal mesh, the edge lengths of the mesh are about the width of the signal trace and all portions of the ground conductor's 6 surfaces are discretized using same edge length as on the signal trace (except on the 4 side surfaces where there are smaller elements). This gives rise to a total of 38 424 triangles of which 1192 are on the signal trace. (ii) In dense mesh, the edge lengths of the signal trace mesh are about half the width of the trace and the mesh density on the ground conductor in the region below the signal trace is also the same. The edge length in other portions of the ground conductor is identical to that in normal mesh. There are a total of 78 432 triangles of which 3570 are on the signal trace. (iii) The very dense mesh is obtained by further refining the dense mesh and reducing the edge length on the signal trace and the portion of the ground conductor below it to about 1/3 of the signal trace width. There are now three regions of increasingly finer meshes on the ground plane for a total of 109 564 triangles of which 17 274 are on the signal trace. For comparison, a typical automatically and adaptively-computed mesh from a commercial software based on the finite-element method (FEM), obtained by setting the meshing frequency to 20 GHz and using default parameters for all mesh settings is shown in Fig. 2(d). Note the density of the mesh on the top and side surfaces of the signal trace and the ground conductor under it.

#### A. SOC deembedding

In this article, the non-radiating lumped-port model in [8] is used to excite/terminate the microstrip line and extract network parameters; the model uses testing and basis functions with supports over disconnected triangles. While pairs of triangles, one on the signal trace and the other on the ground plane, are used for the typical LMIE approach's (finite ground model) port, a single triangle on the signal trace is used in the reduced-domain LMIE approach's (infinite ground plane model) port.

First, the  $S$ -parameters are obtained directly, without any de-embedding techniques, using the normal mesh; the results are shown in Fig. 3 (dashed lines): While the  $S_{11}$  shows good agreement below 5 GHz, it differs significantly in the rest of the frequency range. Next, the effect of the lumped-port models is removed by using the SOC de-embedding technique [9]. During de-embedding, 150-um long feed lines were attached at each port for the typical LMIE approach; this did not yield consistent results for the reduced-domain LMIE approach and the feed lines were extended to 610 um at each port. This decreased the magnitude of  $S_{11}$  from both approaches in Fig. 3 (solid lines). This result is to be expected because the microstrip line is designed to 50  $\Omega$  termination and reference impedance for the  $S$ -parameters is also 50  $\Omega$ . Somewhat surprisingly, while good agreement is still observed below 5 GHz, the difference between the results of the two LMIE approaches *increases* above 5 GHz after de-embedding. As an independent check,  $S_{11}$  is also computed using the commercial FEM-based software with the mesh in Fig. 2(d) and using the wave-port model; this yields yet another result that is different from both LMIE computations and fails to explain the difference.

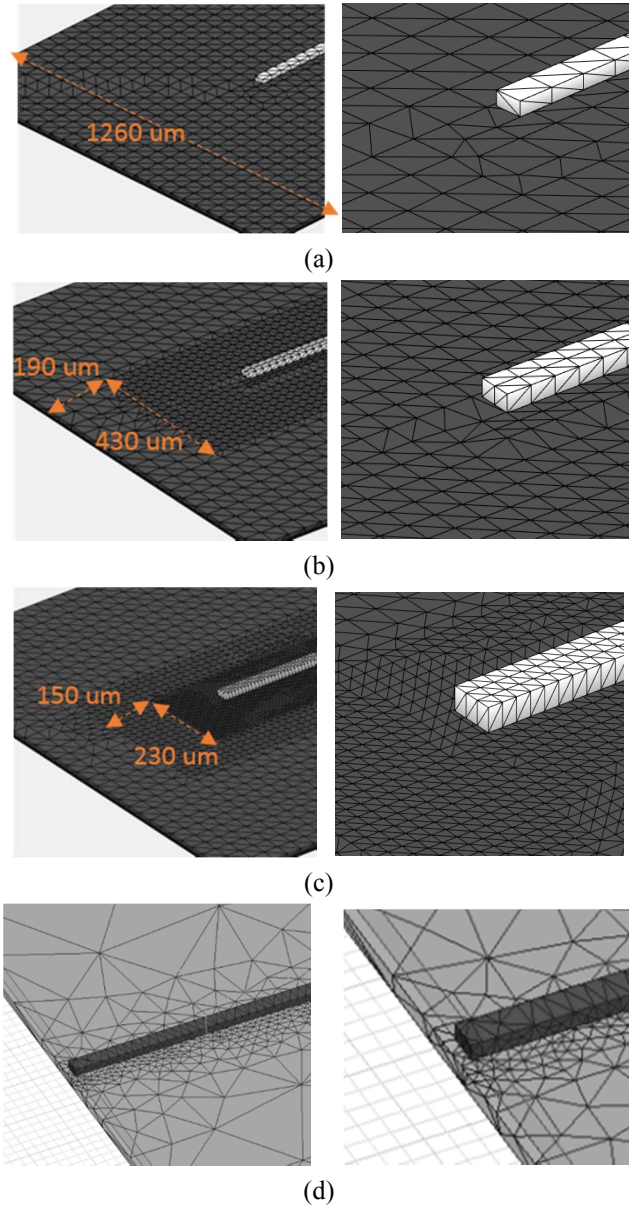


Fig. 2. The various meshes used in this article. The (a) normal mesh, (b) dense mesh, and (c) very-dense mesh used in the LMIE computations (only the signal line portion of the mesh is used in the reduced-domain LMIE approach). Also shown is (d) the surface portion of a typical volumetric mesh generated using a commercial FEM software. The right figures are the same as the left ones, but zoomed in near the end of the signal line.

#### B. Reduced-Domain LMIE

In this approach, the ground reference is incorporated into layered-medium Green's function as an infinite plane but with finite thickness and conductivity [1]; this removes the need to discretize the current on the reference conductor (simplifying meshing), reduces the number of unknowns to only those assigned to signal traces, and can yield better conditioned systems of equations [1]. On the other hand, introducing a highly-conductive layer to the background medium complicates the accurate computation of layered-medium Green's functions. To ameliorate this issue, log- and linear-scale interpolation [7] are used for near-singular and other interactions, respectively.

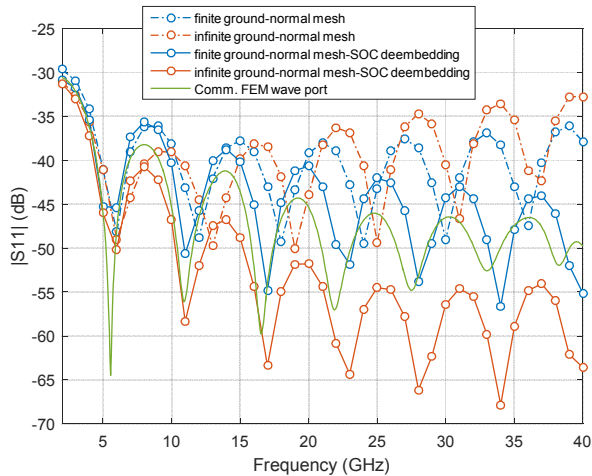


Fig. 3. S11 computed using the two LMIE approaches without any deembedding and S11 computed by SOC deembedding of the results of the two LMIE approaches compared to that from an FEM solver.

### B. Increasing mesh density

To evaluate the convergence of the results, the denser meshes in Figs. 2(b) and 2(c) are used and the results obtained from LMIE computations are shown in Fig. 4. In both approaches, as the mesh is refined, the magnitude of S11 further decreases and becomes closer to each other; the change is especially significant for the typical LMIE approach using the finite-ground model. Clearly, the normal mesh is not sufficient to obtain an accurate S11 parameter for the typical LMIE approach in this benchmark signal line with a well-matched port. Fig. 4 shows that the typical LMIE approach requires the very dense mesh whereas the reduced-domain LMIE approach requires only the dense mesh to obtain highly accurate S11 results; i.e., they require 171 084 and 11 590 RWG functions, respectively.

## IV. CONCLUSION

Two LMIE approaches were compared using a package-scale benchmark microstrip line. While the ground reference is modeled as a finite conductor in the typical LMIE approach, it is modeled as an infinite conductor and incorporated into the Green's function in the reduced-domain LMIE approach. The S11 parameters computed by the two approaches were found to be different even after a de-embedding technique was applied. Using increasingly denser meshes showed that the reduced-domain LMIE method produced more accurate results for the same mesh density on the signal trace.

The results indicate that in order to obtain a highly accurate S11 parameter for this benchmark problem, it is important to also accurately model the currents on the ground plane; i.e., regions on reference planes near the signal trace should also be carefully/densely discretized. Indeed, while the mesh density on signal traces is generally considered significant for accuracy, the mesh density on the ground plane can also affect the accuracy of the results for methods that discretize currents on/in reference planes. Because multi-layer electronic packages generally have multiple ground and power planes, the mesh density on these planes can be a serious impediment for typical LMIE methods, increasing their computational costs significantly. This article

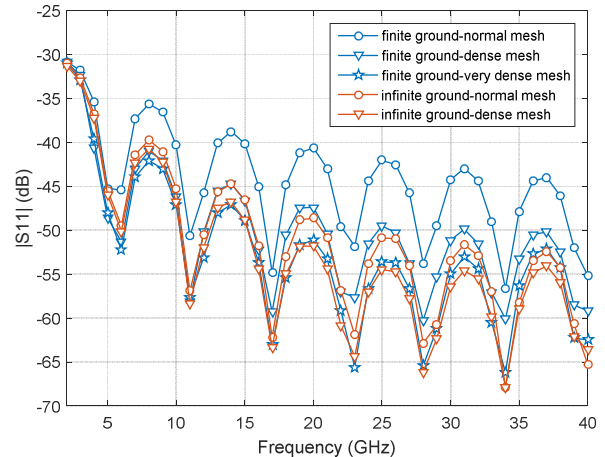


Fig. 4. S11 computed with the typical LMIE approach and the reduced-domain LMIE approach using different mesh densities (all of S11 are computed by SOC deembedding).

shows that reduced-domain LMIE methods can not only reduce the computational costs but also potentially provide more accurate results by modeling these planes using Green's functions.

## ACKNOWLEDGMENT

This research was supported by Intel Corporation. The authors thank M. Shattuck from Cadence-AWR for suggesting this study and the Texas Advanced Computing Center for providing HPC resources that have contributed to the research results reported within this article.

## REFERENCES

- [1] C. Liu and A. E. Yilmaz, "A reduced-domain layered-medium integral-equation method for electronic packages," in *Proc. IEEE 28th Conf. Elect. Perform. of Electron. Packag. Syst. (EPEPS)*, 2019.
- [2] B. Wu and L. Tsang, "Fast computation of layered medium Green's functions of multilayers and lossy media using fast all-modes method and numerical modified steepest descent path method," *IEEE Trans. Microw. Theory Tech.*, vol. 56, no. 6, pp. 1446–1454, June 2008.
- [3] Z. Song, H.-X. Zhou, K.-L. Zheng, J. Hu, W.-D. Li and W. Hong, "Accurate evaluation of Green's functions for a lossy layered medium by fast extraction of surface- and leaky-wave modes," *IEEE Antennas Propag. Mag.*, vol. 55, no. 1, pp. 92–102, Feb. 2013.
- [4] C. Liu, K. Aygun, and A. E. Yilmaz, "A parallel FFT-accelerated layered-medium integral-equation solver for electronic packages," *Int. J. Num. Model.: Electron. Networks, Dev., Fields*, vol. 33, no. 2, 2020.
- [5] S. M. Rao, D. R. Wilton, and A. W. Glisson, "Electromagnetic scattering by surfaces of arbitrary shapes," *IEEE Trans. Antennas Propag.*, vol. 30, no. 3, pp. 409–418, May 1982.
- [6] E. Şimşek, Q. H. Liu, and B. Wei, "Singularity subtraction for evaluation of Green's functions for multilayer media," *IEEE Trans. Microw. Theory Tech.*, vol. 54, no. 1, pp. 216–224, Jan. 2006.
- [7] H. Yang and A. E. Yilmaz, "A log-scale interpolation method for layered medium Green's function," in *Proc. IEEE Antennas Propag. Soc. Int. Symp.*, July 2018.
- [8] C. Liu, J. W. Massey, and A. E. Yilmaz, "A nonradiating finite-gap lumped-port model," *IEEE Antennas Wireless Propag. Lett.*, vol. 17, no. 7, pp. 1339–1343, July 2018.
- [9] L. Zhu and K. Wu, "Unified equivalent-circuit model of planar discontinuities suitable for field theory-based CAD and optimization of M(H)MIC's," *IEEE Trans. Microw. Theory Tech.*, vol. 47, no. 9, pp. 1589–1602, Sep. 1999.